Green Chemistry

COMMUNICATION

View Article Online
View Journal | View Issue

Check for updates

Cite this: *Green Chem.*, 2021, **23**, 745

Received 30th November 2020,
Accepted 24th December 2020

DOI: 10.1039/d0gc04054a

rsc.li/greenchem

Unexpected selective alkaline periodate oxidation of chitin for the isolation of chitin nanocrystals†

Peiwen Liu, ‡[a] Huan Liu, ‡[a] Timmy Schäfer,[b] Torsten Gutmann,[b] Holger Gibhardt,[c] Houjuan Qi,[a,d] Lin Tian,[e] Xizhou Cecily Zhang,[f] Gerd Buntkowsky[b] and Kai Zhang *[a]

Periodate oxidation reaction occurring directly on chitin has been neglected in polysaccharide chemistry so far. Herein, we present the first direct alkaline periodate oxidation of chitin, which demonstrates at the same time a novel approach for the preparation of chitin nanocrystals (ChNCs). This oxidation is based on an unprecedented selective reaction of non-ordered domains of chitin by the dimeric orthoperiodate ions ($H_2I_2O_{10}^{4-}$) as the major species in alkaline surroundings. Nearly 50 wt% of non-ordered regions are dissolved after sequential accelerated partial deacetylation, periodate oxidation and β-alkoxy fragmentation, which allows the isolation of up to 50 wt% of uniform anisotropic zwitterionic ChNCs.

Periodate can selectively cleave the carbon–carbon bonds of a variety of 1,2-difunctionalised alkanes and introduce aldehyde groups,[1] which makes it an increasingly viable tool in carbohydrate chemistry for promising applications.[2–6] Despite the tremendous progress made in the utilization of chitin over the past decades, periodate oxidation remained absent from the toolbox for the direct modification of chitin. This is primarily due to the fact that the *N*-acetylation of the amino groups prevents the cleavage of C–C bonds between C2 and C3 by metaperiodate oxidation.[7,8] To allow the periodate oxidation on the amino group at C2 position and the hydroxyl group at C3 position (Fig. 1), a high degree of deacetylation of chitin is required.[9,10] Typically, deacetylated chitin that is suitable for periodate oxidation has a degree of deacetylation above 80%, which is known as chitosan.[11,12] During the deacetylation, most of the ordered domains of chitin are converted to the non-ordered state.[13] Thereafter, chitosan generally undergoes the periodate oxidation in acidic surroundings and is converted into water-soluble dialdehyde chitosan (Fig. 1).[11,14] So far, no report about direct periodate oxidation of chitin is known and it is generally accepted that the periodate oxidation is only accessible to chitosan as highly deacetylated chitin or the deacetylated sites on chitin chains.[7,8,14–16]

However, according to the current progress in periodate oxidation,[17] the alkaline environment of the newly found alkaline periodate oxidation provides the possibility to complete the deacetylation and periodate oxidation of chitin in a one-pot process. Considering the low reaction probability of alkaline periodate oxidation on highly ordered cellulose,[17] we envisioned the possibility to produce ChNCs as the isolated highly ordered domains of chitin by alkaline periodate oxidation due to the comparable chemical and physical structures of native cellulose and chitin.[18–20] With the important properties of chitin and the advantages of nanoparticles,[21–23] ChNCs can address the limitations of chitin in terms of solubility, reactivity, and processability. To date, several classic approaches have been developed, which generally include acid hydrolysis,[23] TEMPO-mediated oxidation,[24] ammonium persulfate method,[25] and partial deacetylation.[26] However, due to the financial risks associated with ChNC production,[27] ChNCs have not been widely used. Thus, with the selectivity of alkaline periodate oxidation and the characteristic that periodate can be cost-efficiently regenerated from iodate under alkaline conditions,[6,17,28] it should be very attractive in the production of ChNCs *via* alkaline periodate oxidation from the massive amount of bio-waste accumulated by marine-capture fisheries, food industry or other resources (up to 10 gigatons chitin per year).[27]

[a]*Department of Wood Technology and Wood-based Composites, Georg-August-University of Göttingen, Büsgenweg 4, D-37077 Göttingen, Germany. E-mail: kai.zhang@uni-goettingen.de*
[b]*Eduard-Zintl-Institute for Inorganic Chemistry and Physical Chemistry, Technical University Darmstadt, Alarich-Weiss-Straße 4, D-64287 Darmstadt, Germany*
[c]*Institute of Physical Chemistry, Georg-August-University of Göttingen, Tammannstrasse 6, D-37077 Göttingen, Germany*
[d]*Key Laboratory of Bio-based Material Science & Technology (Northeast Forestry University), College of Materials Science and Engineering, Ministry of Education, Harbin 150040, China*
[e]*Institute of Materials Physics, Georg-August-University of Göttingen, Friedrich-Hund-Platz 1, 37077 Göttingen, Germany*
[f]*NMR-based Structural Biology, Max-Planck-Institute for Biophysical Chemistry, Am Fassberg 11, 37077 Göttingen, Germany*

†Electronic supplementary information (ESI) available. See DOI: 10.1039/d0gc04054a

‡These authors contributed equally to this work.

Open Access Article. Published on 24 December 2020. Downloaded on 2/13/2026 11:01:19 AM.
This article is licensed under a Creative Commons Attribution-NonCommercial 3.0 Unported Licence.

Open Access Article. Published on 24 December 2020. Downloaded on 2/13/2026 11:01:19 AM.
This article is licensed under a Creative Commons Attribution-NonCommercial 3.0 Unported Licence.

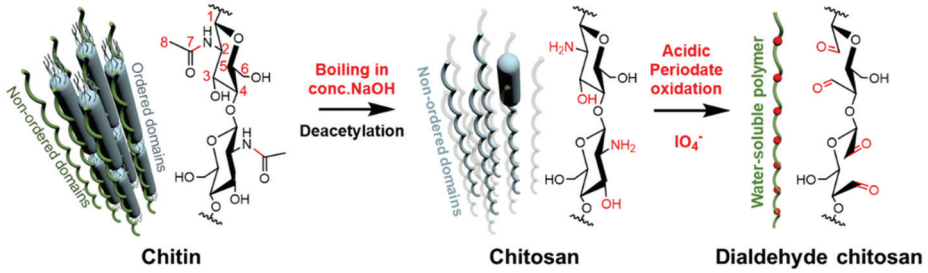

Fig. 1 Previously reported general process of the acidic periodate oxidation of chitosan as highly deacetylated chitin.[11,14,16,17,29]

In the present work, we show the unexplored periodate oxidation on chitin in alkaline media, which selectively attacks the non-ordered domains of chitin in a one-pot process through a starting weak deacetylation and subsequent efficient oxidation of deacetylated glucosamine units of low quantities. After further hydrolysis of oxidized chitin chains in non-ordered domains, homogeneous anisotropic zwitterionic ChNCs (referred to as PO-ChNCs) in high yields are obtained.

The typical alkaline periodate oxidation at pH 10 at room temperature performed as a one-pot reaction is shown in Fig. 2A. To accelerate the diffusion of alkaline periodate in chitin, 1 g of chitin was soaked in 3 wt% KOH solution at room temperature for 24 h as pre-treatment to swell and to partially cleave the hydrogen bonds in the non-ordered domains. To prevent the settlement of periodate ions and ensure the existence of sufficient periodate ions in the reaction solution,[17] an excess of 7 g of orthoperiodic acid (H_5IO_6) was added to oxidize chitin and the pH value was adjusted to 10 with an aqueous KOH solution. The reaction mixture was stirred for 14 days with the exclusion of light to prevent the formation of radicals.[30] After separation and purification, nearly 50 wt% of chitin was converted into soluble compounds. The remaining solid part was obtained as a stable suspension.

It should be noted that, according to conventional wisdom in chitin chemistry, the deacetylation is extremely slow for chitin in such a mild alkaline environment of pH 10.[9,21,31] In order to accelerate the deacetylation and reduce the use of mineral bases, alkaline deep eutectic solvents were used in some recent studies.[32–34] In our experiment, the degree of deacetylation of chitin remained below 10% and did not increase significantly even after soaking in a buffer at pH 10 or aqueous KOH (3 wt%) for 14 days (Fig. S1†). This low concentration of deacetylated sites is generally regarded to be too low for the periodate oxidation of chitin.[11,16]

In contrast to previous findings, the addition of potassium dimeric orthoperiodate in the alkaline solution at pH 10 significantly promoted sequential reactions as accelerated deacetylation, oxidation, and degradation, which converted chitin to soluble compounds (Fig. 2B). As shown above and in Fig. S1,† the mild alkaline reaction environment (pH 10) and soaking should have enhanced the accessibility of chitin by breaking the hydrogen bonds.[35] The deacetylated sites along chitin chains were then further oxidized, resulting in a C2–C3 bond cleavage and the formation of dialdehydes. Unlike the dialdehyde chitosan that is generally obtained after the acidic periodate oxidation on chitosan,[11,14] these oxidized chitin chains further undergo a rapid β-alkoxy fragmentation[36] of the C5–O5 bonds and Cannizzaro reaction due to the presence of an alkaline environment.[36] Following the β-alkoxy fragmentation, the chitin chains were broken and the chitin particles became smaller (Fig. S2†). After further periodate oxidation and degradation in an alkaline environment, ammonium acetate,[37] potassium acetate[38] and potassium formate[17] were formed among other low-molecular-weight compounds of minor amounts (detailed reactions in Fig. S3†), according to their ^{1}H and ^{13}C NMR spectra (Fig. 2C and S4†). This shows that chitin chains were removed from the raw bulk chitin, which increased the exposed surface for further reactions (Fig. S2†).[24,39]

In addition, the deacetylation of chitin at pH 10 was significantly accelerated during the alkaline periodate oxidation, compared with the slow and limited deacetylation in alkaline solutions at pH 10 without periodate (Fig. 2D and S1†). In the first 24 h, 23 ± 5 wt% of chitin was deacetylated and oxidized (Fig. 2D, the mass loss in Fig. 2 refers to the difference between the amount of total solids and the amount of raw materials). The deacetylation rate of chitin was then slowed down, and the oxidation of chitin almost reached a steady state after 14 days of reaction, as demonstrated by the small mass loss (<4 wt%) in the period between 14 and 30 days of reaction (Fig. 2D).

Therefore, the periodate oxidation on deacetylated glucosamine units and their further conversion into soluble compounds promoted further deacetylation of chitin by removing the obtained amine groups along the chitin chains. The amount of deacetylation after a reaction time of 14 days (see Fig. 2E) depends strongly on the pH value. The strongest enhancement of the deacetylation rate and a conversion of 46 ± 3 wt% is found at pH 10. This high efficacy is attributed to the oxidation mediated by dimeric orthoperiodate ions ($H_2I_2O_{10}^{4-}$), which are the major iodine-containing ion species (Fig. 2E and F) at this pH. In contrast, at the lower pH 7.5, only *ca.* 15 wt% is converted, despite the stronger oxidation capacity of monoanionic periodate ($H_4IO_6^-$) (Fig. S5†).[1,17] We attribute this effect as a result of the very low concentration of hydroxide ions (OH^-) at pH 7.5, which limits the sequential reactions, because no sufficient deacetylated sites could be provided to

 This journal is © The Royal Society of Chemistry 2021

Open Access Article. Published on 24 December 2020. Downloaded on 2/13/2026 11:01:19 AM.
This article is licensed under a Creative Commons Attribution-NonCommercial 3.0 Unported Licence.

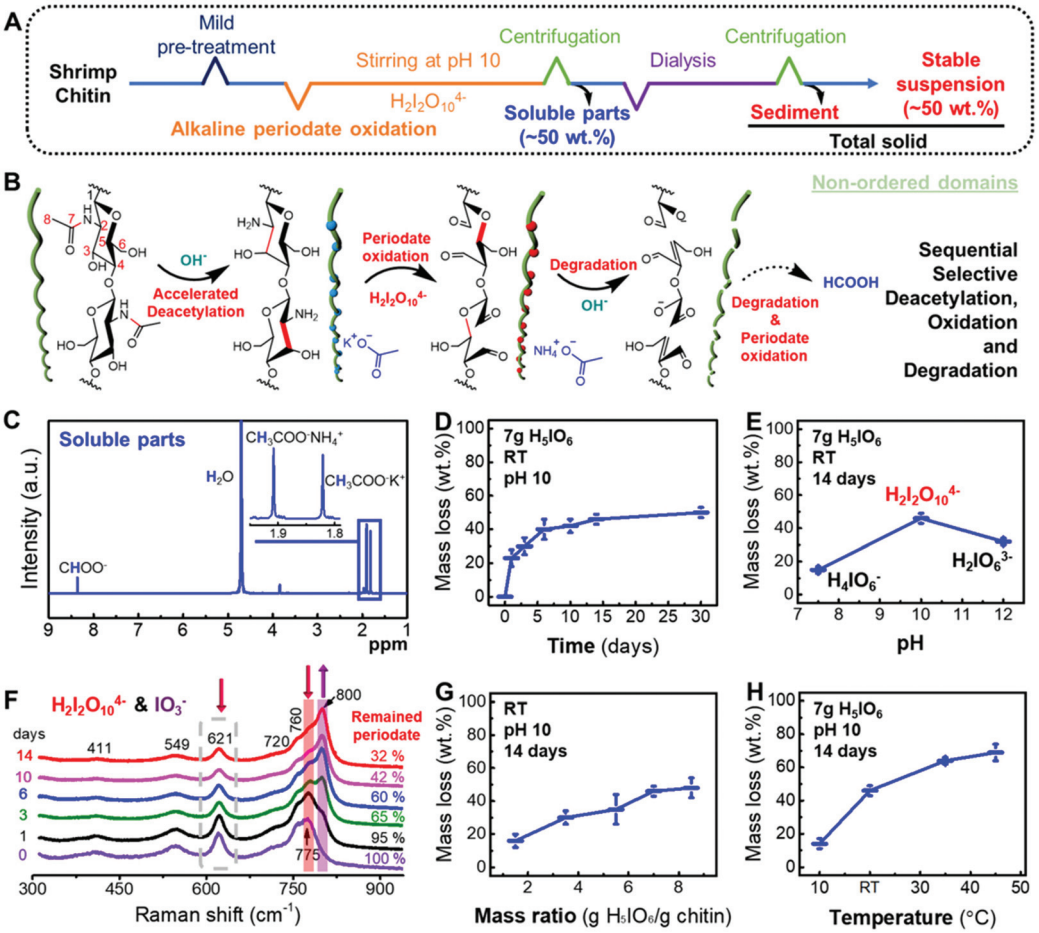

Fig. 2 The alkaline periodate oxidation of chitin. (A) Flow diagram for the alkaline periodate oxidation of chitin at pH 10. (B) Proposed pathway for the accelerated deacetylation, oxidation of chitin in non-ordered domains, and further degradation resulting in soluble compounds. (C) ^{1}H NMR spectra of soluble compounds from alkaline periodate oxidation of chitin in D_2O. (D) Mass loss of chitin during 30 days of reaction. (E) Effect of pH values on the alkaline periodate oxidation of chitin. (F) Representative Raman spectra of the solution showing the remaining concentrations of iodine-containing anions as a function of the reaction time in days (note the starting spectrum at 0 day is the Raman spectrum of the solution before adding chitin). (G) Effect of periodate amount used for alkaline periodate oxidation. (H) Effect of reaction temperature on the alkaline periodate oxidation of chitin.

initiate the oxidation and the following reactions. At the higher pH 12, a conversion of 32 ± 2 wt% is observed. Since at this pH periodate ions are present as trianionic periodate ($H_2IO_6^{3-}$) (Fig. S5†) and not as orthoperiodate ions ($H_2I_2O_{10}^{4-}$), we conclude that the presence of sufficient amounts of $H_2I_2O_{10}^{4-}$ ions is a critical parameter for the efficient alkaline periodate oxidation of chitin.

In addition, a larger amount of periodate (8.5 g H_5IO_6 per gram of chitin) resulted in similar mass loss compared to the oxidation using 7 g of periodic acid. This implies that 7 g of periodic acid is sufficient for the alkaline periodate oxidation of chitin (Fig. 2F and G). To elucidate the reaction mechanism, the amounts of $H_2I_2O_{10}^{4-}$ ions were monitored during the 14 days of reaction by Raman spectroscopy. The intensities of the peaks at 621 and 760 cm^{-1} attributed to the $H_2I_2O_{10}^{4-}$ ions[17,40] strongly decreased with a longer reaction time (Fig. 2F and S6†). A new peak at 800 cm^{-1} was attributed to the iodate ions (IO_3^-)[41] that appeared after 24 h of reaction and increased strongly with a longer reaction time up to 14 days. After 14 days, the amount of periodate remaining in the solutions was 32 wt% of the initial amount. Theoretically, fully deacetylated chitin (0.0049 mol) obtained from 1 g of chitin would only need 1.12 g of orthoperiodic acid for complete oxidation.[1] Thus, the consumption of 4.8 g orthoperiodate for around 0.5 g mass loss of chitin indicates that a significant amount of orthoperiodate was depleted for side reactions, *e.g.* the oxidation of the products from β-alkoxy fragmentation (Fig. S3†).

Fig. 2H displays the temperature dependence of the alkaline periodate oxidation after 14 days between 10 °C and 45 °C. The reaction reveals a typical Arrhenius type temperature activation (see Fig. S7†) with an activation energy of 22.1 kJ mol^{-1} K^{-1}, *i.e.* enhanced deacetylation and oxidation process by heating.[1,9]

As revealed before on cellulose,[2,17] the alkaline periodate oxidation should predominantly selectively remove the non-

Open Access Article. Published on 24 December 2020. Downloaded on 2/13/2026 11:01:19 AM.
This article is licensed under a Creative Commons Attribution-NonCommercial 3.0 Unported Licence.

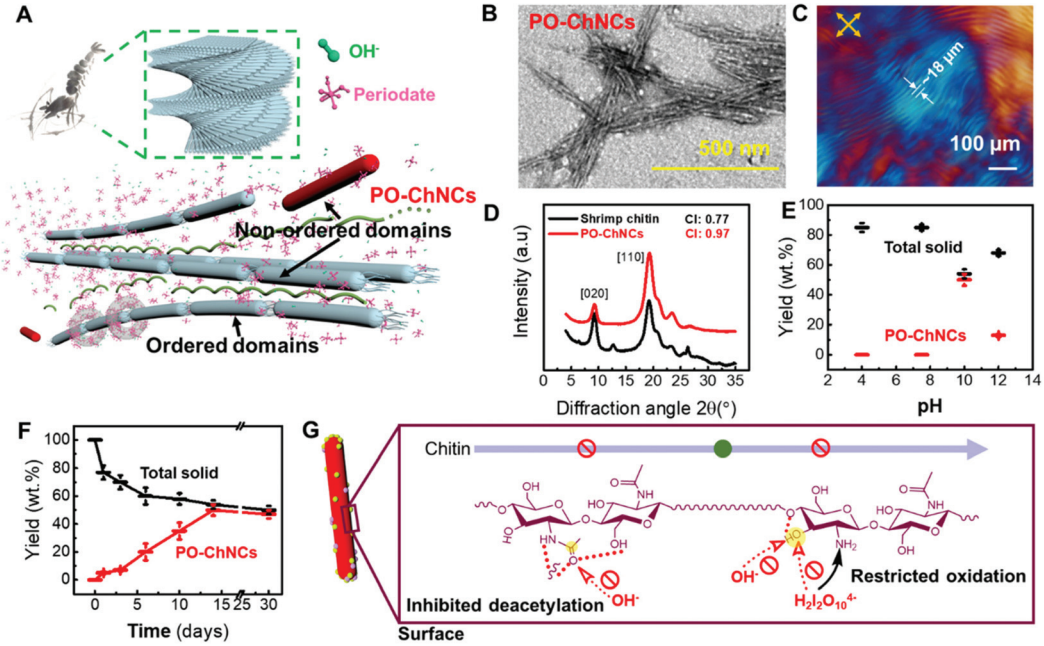

Fig. 3 Isolation of PO-ChNCs by selective alkaline periodate oxidation of non-ordered domains of chitin. (A) Schematic representation of the production of PO-ChNCs by selective alkaline periodate oxidation of the non-ordered chitin domains. (B) TEM image of the obtained PO-ChNCs from shrimp chitin. (C) Polarized optical microscopy image of a typical fingerprint pattern of the cholesteric phase of an aqueous suspension of PO-ChNCs (6 wt%). (D) X-ray diffraction patterns and crystallinity index (CI) of the shrimp chitin and PO-ChNCs. (E) and (F) Development of yields of PO-ChNCs and total solids depending on the pH value and reaction time, respectively. (G) Schematic representation of the restricted deacetylation and alkaline periodate oxidation of PO-ChNCs.

ordered domains of chitin (Fig. 3A). In fact, the remaining solid part in the supernatant after the reaction at pH 10 at room temperature was mainly PO-ChNCs, representing the isolated ordered domains of chitin (Fig. 3B). Uniform PO-ChNCs exhibited a typical needle-like morphology according to the TEM measurements. Equilibrated PO-ChNC suspensions in a square quartz tube showed the fine fingerprint pattern of cholesteric phase (Fig. 3C).

The DNP enhanced $^{1}H \rightarrow {}^{13}C$ CP NMR spectra of PO-ChNCs and the raw shrimp chitin contain signals at similar chemical shifts between 0 and 200 ppm, which were attributed to each carbon atom of chitin chains (Fig. S8 and S9†). Therefore, chitin chains are still the only building blocks of the remaining solid parts, after the alkaline periodate oxidation. Despite the same chemical compositions, XRD spectra of PO-ChNCs showed an increase of the crystallinity index from 0.77 to 0.97 after 14 days of reaction, compared to the raw shrimp chitin (Fig. 3D). The crystallinity index was calculated from the peak intensity I_{110} and the baseline intensity $I_{amorphous}$ at the diffraction angles of 19.6° and 16.0°, respectively.[24] The crystal sizes of the [020] and [110] directions were calculated according to the Scherrer equation.[24] With the widths at half-heights of the diffractions peaks at 9.6° and 19.6°, the crystal sizes of the [020] and [110] directions in shrimp chitin were 8.77 nm and 6.68 nm, and the crystal sizes of the [020] and [110] directions in PO-ChNCs were 9.02 nm and 6.53 nm, respectively. Therefore, the non-ordered domains in chitin that connected the ordered domains of chitin should have been mainly eliminated during the 14 days of alkaline periodate oxidation, releasing the ordered domains as PO-ChNCs. This fact further verified the selective reaction of the alkaline periodate oxidation.

Accordingly, the pH dependence of the PO-ChNC concentration after 14 days (Fig. 3E) exhibits a similar trend as that shown in Fig. 2E with a maximum around pH 10, where the concentration of $H_2I_2O_{10}^{4-}$ is highest. Moreover, the yield of PO-ChNCs did not significantly change by extending the reaction time for the alkaline periodate oxidation from 14 to 30 days (Fig. 3F), corroborating the result from Fig. 2D. It is notable that periodate oxidation with sodium metaperiodate ($NaIO_4$) did not result in ChNCs in our control experiments (Fig. 3E). Furthermore, the effects of the reaction temperature and the amount of periodate on the isolation process were studied to obtain the optimum condition for producing the maximum amount of chitin nanocrystals with the minimum time (Fig. S10†). Ambient temperature and 7 g of periodate would be sufficient to isolate the maximum amount of PO-ChNCs from 1 g of chitin.

The PO-ChNCs exhibited a much better stability in the reaction solution as raw shrimp chitin at pH 10 and 30 wt% periodate concentration in the reaction solution. After 14 days of reaction, the PO-ChNCs underwent a weight loss of only ~10 wt%, while the raw shrimp chitin exhibited a weight loss of about 50 wt% after 14 days of reaction (Fig. S11†).

 This journal is © The Royal Society of Chemistry 2021

Open Access Article. Published on 24 December 2020. Downloaded on 2/13/2026 11:01:19 AM.
This article is licensed under a Creative Commons Attribution-NonCommercial 3.0 Unported Licence.

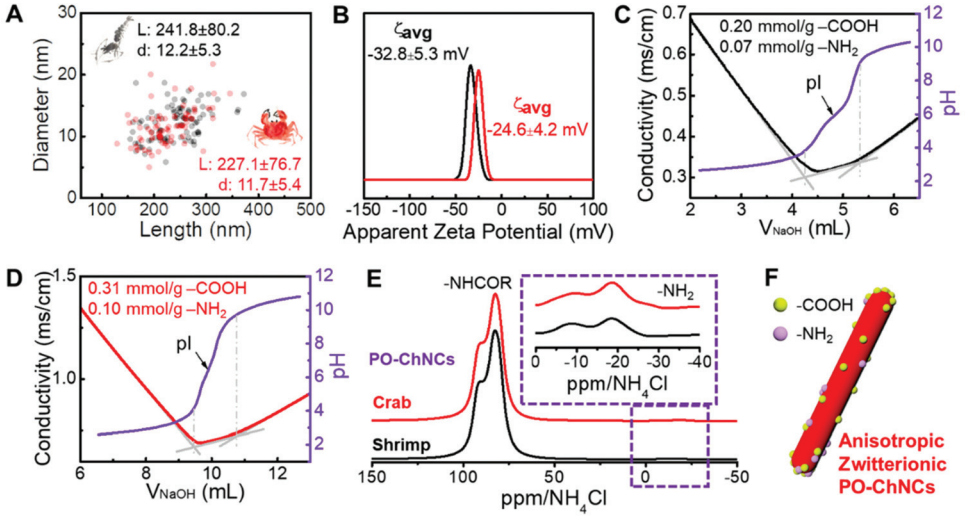

Fig. 4 Anisotropic zwitterionic PO-ChNCs obtained from the 14-day one-pot alkaline periodate oxidation of shrimp and crab chitin. (A) Size distribution of PO-ChNCs based on TEM measurements. Red symbols represent the crab PO-ChNCs and black symbols represent the shrimp PO-ChNCs. (B) Zeta potentials of PO-ChNCs. (C) and (D) Conductivity titration curves of PO-ChNC suspensions with aqueous NaOH solution (0.05 M). pI represents the isoelectric point. (E) DNP enhanced solid-state $^{1}H \rightarrow {}^{15}N$ CP MAS NMR spectra of PO-ChNCs. (F) Schematic representation of anisotropic zwitterionic PO-ChNCs.

This higher stability can be attributed to the strongly restricted deacetylation and cyclisation on the surface of PO-ChNCs in alkaline periodate oxidation at room temperature (Fig. 3G). The deacetylation of PO-ChNCs is strongly inhibited by inter- and intramolecular hydrogen bonds on oxygen and nitrogen in the acetamido groups as well as the steric hindrance (Fig. 3G).[18,42] As soon as a few of the acetamido groups are converted into amine groups on the surface of PO-ChNCs, the alkaline periodate oxidation is also restricted, as revealed before on cellulose nanocrystals.[17] The reason is believed to be the C3-hydroxyl groups of chitin chains in the ordered domains being generally blocked due to their integration in numerous hydrogen bonds (Fig. 3G).[18,43] The cyclisation between periodate ions, hydroxyl groups and amine groups for oxidation is subjected to general acid–base catalysis, which requires activated hydroxyl groups on C2 or C3.[17,44] In alkaline periodate oxidation, OH^- will activate the protons in hydroxyl groups on C2 or C3 (Fig. S12†). However, the activation of the blocked protons at the C3-hydroxyl groups is restricted and the cyclisation between hydroxyl groups, amine groups, and periodate ions is therefore highly hampered on the surface of PO-ChNCs.

In addition to shrimp chitin, crab chitin was also used as a substrate to prepare PO-ChNCs to demonstrate the versatility of our method. Nearly 40 wt% of PO-ChNCs was obtained after the alkaline periodate oxidation at pH 10 in an ambient environment. The dimensions of PO-ChNCs from shrimp chitin and crab chitin are distributed within a narrow range (Fig. 4A). Shrimp PO-ChNCs have an average length of 241.8 ± 80 nm, and their average diameter is 12.2 ± 5 nm. Crab PO-ChNCs have a similar average length and diameter of 227.1 ± 76 nm and 11.7 ± 5 nm, respectively.

The change in the pH values of the PO-ChNC suspensions from 10 to ~4 after dialysis and the negative apparent zeta potentials indicate the formation of cationic moieties on their surface. The apparent zeta potential of PO-ChNCs from shrimp chitin was measured to be −32.8 ± 5.3 mV, and −24.6 ± 4.2 mV for PO-ChNCs from crab chitin (Fig. 4B).

These PO-ChNCs contain carboxyl groups on their surface, as verified using conductivity titration (Fig. 4C and D). After 14 days of reaction, the amount of carboxyl groups on the PO-ChNC surface was determined to be 0.20 ± 0.04 mmol g^{-1} on shrimp PO-ChNCs and 0.31 ± 0.03 mmol g^{-1} on crab PO-ChNCs (Fig. 4C and D). The aldehyde groups normally generated from periodate oxidation[8] were not found on PO-ChNCs according to the conductivity titration for aldehyde groups after the reaction with hydroxylamine hydrochloride. The existence of carboxyl groups instead of aldehyde groups on PO-ChNCs is in good agreement with the proposed sequential reaction mechanism in Fig. 2B. The β-alkoxy fragmentation, Cannizzaro reaction, and further oxidation led to the conversion of the aldehyde groups into carboxyl groups (detailed reactions in Fig. S13†).

Furthermore, the low reaction probability of alkaline periodate oxidation on the ordered domains still allows the existence of amino groups on PO-ChNCs. The existence of amine groups on PO-ChNCs was confirmed by DNP enhanced $^{1}H \rightarrow {}^{15}N$ CP MAS NMR (Fig. 4E). In the region of amine nitrogen (−40 to 0 ppm), two signals are observed for crab and shrimp PO-ChNCs (Fig. 4E). The concentration of amino groups on the PO-ChNC surface was determined to be 0.07 ± 0.01 mmol g^{-1} on shrimp PO-ChNCs and 0.10 ± 0.05 mmol g^{-1} on crab PO-ChNCs (Fig. 4C and D). Thus, the production of anisotropic

Open Access Article. Published on 24 December 2020. Downloaded on 2/13/2026 11:01:19 AM.
This article is licensed under a Creative Commons Attribution-NonCommercial 3.0 Unported Licence.

zwitterionic PO-ChNCs from diverse raw chitins was realized by a one-pot reaction for the first time (Fig. 4F).

As a novel method to prepare uniform size-distributed ChNCs, the alkaline periodate oxidation has advantageous features and thus demonstrates a promising method, compared to other existing methods, such as acid hydrolysis,[45] partial deacetylation,[26] (2,2,6,6-tetramethylpiperidin-1-yl)oxyl (TEMPO)-mediated oxidation,[24] ionic liquids solvolysis[46] and ammonium persulfate (APS) oxidation.[25] The detailed comparison is listed in Table S1.† On comparing the most important features of this method with others it is clear this method does not require heating which is essential for the methods of acid hydrolysis, partial deacetylation, APS oxidation and ionic liquids solvolysis. This method also does not need corrosive concentrated acids and concentrated bases, in contrast to the acid hydrolysis and partial deacetylation. Moreover, the simple isolation process avoids extensive operation, which is required for the methods of partial deacetylation and TEMPO-mediated oxidation.[47] Besides, the alkaline periodate oxidation generates iodate with very low toxicity. Furthermore, the isolation of ChNCs in our method is performed at ambient temperature and the main power input in the reaction is for the mild stirring (that could also be paused in between).

Besides, Waldvogel's group recently reported the direct and cost-efficient electrochemical synthesis of periodate from iodide and iodate on a large scale, which is less costly and relies on a readily available starting material, such as I^- or IO_3^-.[6] Based on this well-developed electrochemical technology, a feasible protocol can be suggested to deal with the potential environmental issues and high cost of periodate oxidants. The solution containing the periodate and iodate after the isolation of ChNCs can be separated from the solid part and reused for the regeneration of periodate *via* the electrochemical oxidation. The trace amount of periodate, if any, remained in solid products can be regained in the reaction solutions after washing or reduced to potassium iodate by adding ethylene glycol. Therefore, the risk of periodate exposure to the external environments and the cost of periodate can be greatly reduced. Moreover, the 14-day duration of reaction time could be reduced, if we consider the use of additives or applying the pretreatment to accelerate the deacetylation and to partially break the hydrogen bonds in chitin in advance.

Conclusions

Herein we have shown that alkaline periodate oxidation at pH 10 can selectively oxidize and degrade the non-ordered domains of chitin to produce PO-ChNCs. This oxidation is based on a selective reaction of non-ordered domains of chitin by the dimeric orthoperiodate ions ($H_2I_2O_{10}^{4-}$) in alkaline environment. Non-ordered regions are dissolved after sequential accelerated partial deacetylation, periodate oxidation and β-alkoxy fragmentation. The deacetylated sites generated initially at pH 10 allow the alkaline periodate oxidation to selectively remove nearly 50 wt% of the non-ordered domains of chitin during 14 days of reaction. In comparison, the deacetylation and cyclisation are preferentially suppressed on the surface of the ordered domains of chitin, allowing the isolation of up to 50 wt% of uniform anisotropic zwitterionic ChNCs. ChNCs from both shrimp and crab have an average length and width of 220–250 nm and around 12 nm, respectively. Besides, carboxyl groups instead of aldehyde groups are generated on the ChNCs after the β-alkoxy fragmentation, Cannizzaro reaction, and further oxidation. Notable features of our strategy include (1) the first alkaline periodate oxidation of chitin, (2) a novel approach for the isolation of narrowly distributed and anisotropic zwitterionic PO-ChNCs in a one-pot reaction, (3) mechanistic insights into the selectivity of alkaline periodate oxidation of chitin and (4) a proposed route for the alkaline periodate oxidation on non-ordered chitin. The unexpected selective alkaline periodate oxidation of non-ordered domains of chitin broadens the scope of periodate oxidation as well as the available toolbox for chitin exploitation.

Conflicts of interest

There are no conflicts to declare.

Acknowledgements

K. Z. thanks the Federal Ministry for Economic Affairs and Energy (BMWi) and the Ministry for Science and Culture of Lower Saxony (MWK) for the financial support of the WIPANO project (FKZ03THW05K14). P. L. and H. L. thank the China Scholarship Council (CSC) for financial support. We cordially thank Mrs Xiaolin Ding from the University of Göttingen for providing water color paintings of shrimp and crab. T. G. thanks the DFG under contract GU 1650/3-1 for financial support.

References

1 G. Dryhurst, *Periodate oxidation of diol and other functional groups: analytical and structural applications*, Elsevier, 2015.
2 P. Liu, C. Mai and K. Zhang, *ACS Sustainable Chem. Eng.*, 2017, **5**, 5313–5319.
3 H. Yang, M. N. Alam and T. G. van de Ven, *Cellulose*, 2013, **20**, 1865–1875.
4 U.-J. Kim, S. Kuga, M. Wada, T. Okano and T. Kondo, *Biomacromolecules*, 2000, **1**, 488–492.
5 H. Liimatainen, M. Visanko, J. A. Sirviö, O. E. O. Hormi and J. Niinimaki, *Biomacromolecules*, 2012, **13**, 1592–1597.
6 S. Arndt, D. Weis, K. Donsbach and S. R. Waldvogel, *Angew. Chem.*, 2020, **59**, 8036–8041.
7 G. A. Roberts, *Chitin chemistry*, Macmillan International Higher Education, 1992.
8 I. M. Vold and B. E. Christensen, *Carbohydr. Res.*, 2005, **340**, 679–684.

 This journal is © The Royal Society of Chemistry 2021

Open Access Article. Published on 24 December 2020. Downloaded on 2/13/2026 11:01:19 AM.
This article is licensed under a Creative Commons Attribution-NonCommercial 3.0 Unported Licence.

9 P. Sivashankari and M. Prabaharan, in *Chitosan Based Biomaterials Volume 1*, Elsevier, 2017, pp. 117–133.
10 K. Zhang, A. Geissler, S. Fischer, E. Brendler and E. Bäucker, *J. Phys. Chem. B*, 2012, **116**, 4584–4592.
11 H.-L. Jiang, Y.-K. Kim, R. Arote, J.-W. Nah, M.-H. Cho, Y.-J. Choi, T. Akaike and C.-S. Cho, *J. Controlled Release*, 2007, **117**, 273–280.
12 M. N. V. Ravi Kumar, R. A. A. Muzzarelli, C. Muzzarelli, H. Sashiwa and A. J. Domb, *Chem. Rev.*, 2004, **104**, 6017–6084.
13 M. X. Weinhold, J. C. M. Sauvageau, N. Keddig, M. Matzke, B. Tartsch, I. Grunwald, C. Kübel, B. Jastorff and J. Thöming, *Green Chem.*, 2009, **11**, 498–509.
14 X.-W. Shi, X. Yang, K. J. Gaskell, Y. Liu, E. Kobatake, W. E. Bentley and G. F. Payne, *Adv. Mater.*, 2009, **21**, 984–988.
15 S. Keshk, A. M. Ramadan, A. G. Al-Sehemi, A. Irfan and S. Bondock, *Carbohydr. Polym.*, 2017, **175**, 565–574.
16 I. Charhouf, A. Bennamara, A. Abourriche, A. Chenite, J. Zhu and M. Berrada, *Biosensors*, 2014, **16**, 18.
17 P. Liu, B. Pang, S. Dechert, X. C. Zhang, L. B. Andreas, S. Fischer, F. Meyer and K. Zhang, *Angew. Chem.*, 2020, **59**, 3218–3225.
18 V. L. Deringer, U. Englert and R. Dronskowski, *Biomacromolecules*, 2016, **17**, 996–1003.
19 P. Chen, Y. Nishiyama, J.-L. Putaux and K. Mazeau, *Cellulose*, 2014, **21**, 897–908.
20 A. A. Baker, W. Helbert, J. Sugiyama and M. J. Miles, *Biophys. J.*, 2000, **79**, 1139–1145.
21 M. Rinaudo, *Prog. Polym. Sci.*, 2006, **31**, 603–632.
22 J.-B. Zeng, Y.-S. He, S.-L. Li and Y.-Z. Wang, *Biomacromolecules*, 2012, **13**, 1–11.
23 R. Marchessault, F. Morehead and N. Walter, *Nature*, 1959, **184**, 632–633.
24 Y. Fan, T. Saito and A. Isogai, *Biomacromolecules*, 2008, **9**, 192–198.
25 A. A. Oun and J.-W. Rhim, *Carbohydr. Polym.*, 2017, **175**, 712–720.
26 Y. Fan, T. Saito and A. Isogai, *Carbohydr. Polym.*, 2010, **79**, 1046–1051.
27 A. M. Salaberria, J. Labidi and S. C. Fernandes, *Eur. Polym. J.*, 2015, **68**, 503–515.
28 K. Slavica, S. Martin, H. Takashi, R. Walter, R. Thomas and P. Antje, *ChemSusChem*, 2016, **9**, 825–833.
29 K. Kurita, K. Tomita, T. Tada, S. Ishii, S. I. Nishimura and K. Shimoda, *J. Polym. Sci., Part A: Polym. Chem.*, 1993, **31**, 485–491.
30 E.-T. Yun, H.-Y. Yoo, W. Kim, H.-E. Kim, G. Kang, H. Lee, S. Lee, T. Park, C. Lee, J.-H. Kim and J. Lee, *Appl. Catal., B*, 2017, **203**, 475–484.
31 K. L. B. Chang, G. Tsai, J. Lee and W.-R. Fu, *Carbohydr. Res.*, 1997, **303**, 327–332.
32 M. Shimo, M. Abe and H. Ohno, *ACS Sustainable Chem. Eng.*, 2016, **4**, 3722–3727.
33 Q. Ma, X. Gao, X. Bi, Q. Han, L. Tu, Y. Yang, Y. Shen and M. Wang, *Carbohydr. Polym.*, 2020, **230**, 115605.
34 F. A. Vicente, B. Bradić, U. Novak and B. Likozar, *Biopolymers*, 2020, **111**, e23351.
35 Y. Liu, Z. Liu, W. Pan and Q. Wu, *Carbohydr. Polym.*, 2008, **72**, 235–239.
36 P. Calvini, A. Gorassini, G. Luciano and E. Franceschi, *Vib. Spectrosc.*, 2006, **40**, 177–183.
37 M. Kidwai and K. Singhal, *Synth. Commun.*, 2006, **36**, 1887–1891.
38 M. Medycki, L. Latanowicz, J. Jakubas and J. Latosinska, *Mol. Phys. Rep.*, 2003, **37**, 60–66.
39 T. Saito, S. Kimura, Y. Nishiyama and A. Isogai, *Biomacromolecules*, 2007, **8**, 2485–2491.
40 G. J. Buist and J. D. Lewis, *Chem. Commun.*, 1965, 66–67.
41 J. R. Durig, O. D. Bonner and W. H. Breazeale, *J. Phys. Chem.*, 1965, **69**, 3886–3892.
42 P. Sikorski, R. Hori and M. Wada, *Biomacromolecules*, 2009, **10**, 1100–1105.
43 T. Uto, S. Idenoue, K. Yamamoto and J.-i. Kadokawa, *Phys. Chem. Chem. Phys.*, 2018, **20**, 20669–20677.
44 G. J. Buist, C. A. Bunton and W. C. P. Hipperson, *J. Chem. Soc. B*, 1971, 2128–2142.
45 M. Paillet and A. Dufresne, *Macromolecules*, 2001, **34**, 6527–6530.
46 J.-i. Kadokawa, A. Takegawa, S. Mine and K. Prasad, *Carbohydr. Polym.*, 2011, **84**, 1408–1412.
47 D. Klemm, E. D. Cranston, D. Fischer, M. Gama, S. A. Kedzior, D. Kralisch, F. Kramer, T. Kondo, T. Lindström and S. Nietzsche, *Mater. Today*, 2018, **21**, 720–748.